Talanta 88 (2012) 484–489

Contents lists available at SciVerse ScienceDirect

Talanta

journal homepage: www.elsevier.com/locate/talanta

Flow injection analysis of nanomolar silicate using long pathlength absorbance spectroscopy

Jian Ma, Robert H. Byrne*

College of Marine Science, University of South Florida, 140 7th Avenue South, St. Petersburg, FL 33701, United States

ARTICLE INFO

Article history:
Received 6 September 2011
Received in revised form 29 October 2011
Accepted 3 November 2011
Available online 9 November 2011

Keywords:
Flow injection analysis
Nanomolar detection limit
Silicate
Liquid core waveguide
Long pathlength absorbance spectroscopy

ABSTRACT

Determination of silicate at low concentrations (i.e., nanomolar levels) is an important analytical objective for both marine science and the semiconductor industry. Here we report the use of flow injection analysis (FIA) in combination with long pathlength liquid core waveguide (LCW) spectrometry to achieve detection limits for dissolved silica on the order of 10 nM. Sample throughput for the simple, automated analytical apparatus used in this work is 12 h^{-1} at low levels of dissolved silica; this rate can be increased by a factor of three for higher (micromolar) levels of dissolved silica. The analytical protocol is based on the reaction of silicate with ammonium molybdate to form a yellow silicomolybdate complex, which is subsequently reduced to silicomolybdenum blue by ascorbic acid. Optimization of the FIA procedure included consideration of the compositions and concentrations of reagents, volume of the injection loop, flow rate conditions, and lengths of mixing coils. The interference by phosphate was examined and eliminated through addition of oxalic acid. The dissolved silica detection limit of 7.2 nM in pure water is consistent with the strictest standard for the semiconductor industry, and the 9.0 nM detection limit for seawater shows that this analytical method is also suitable for oligotrophic ocean waters. The targeted analytical range of 10 nM to 5 μM can be easily extended to higher concentrations without altering the experimental hardware—i.e., by simply changing flow rates or selecting alternative analytical wavelengths. Compared to previously published LCW-based spectrophotometric methods, this analytical system exhibits improved sensitivity, reduced sample consumption, and higher sample throughput.

1. Introduction

Nitrate, phosphate, and silicate are essential macronutrients. As such, measurements of the concentrations of these nutrients are among the most commonly performed analyses in oceanographic research. While nitrate and phosphate are required nutrients for all phytoplankton, silicate constitutes an additional requirement for siliceous phytoplankton, such as diatoms, which occasionally dominate inorganic carbon sequestration in the upper ocean [1]. Over areas of the tropical and subtropical ocean, silicate in the euphotic zone can be seasonally or chronically depleted to <0.1–0.6 μM [2,3]. At these levels, silicate may constitute a limiting factor for the productivity of diatoms and thereby a limiting control on the export of carbon from the surface ocean [2,3]. Moreover, sensitive silicate analyses are a prerequisite for accurate Si-flux calculations (production and dissolution of silica tests and frustules) and an improved understanding of silicon cycling in regions that have low silicate concentrations, high nutrients, and low chlorophyll (LSi-HNLC), such as the Sub-Antarctic Zone (SAZ) [1,4].

Trace silicate analysis is also important in industries devoted to the production of modern electronic components (e.g., semiconductors), where ultra purified water (UPW) is required for the production of high-quality products. Silicate levels are of special concern with respect to silicon surface reactions and therefore need to be sensitively and accurately measured at nanomolar levels [5].

Spectrophotometric silicate analyses are most commonly based on reactions with molybdenum salts in an acidic medium to form a yellow silicomolybdic complex (SiMY). SiMY can be measured directly or it can be reduced to silicomolybdenum blue (SiMB). The analytical procedures leading to spectrophotometric detection of SiMB constitute the standard protocol for determination of dissolved silica [6–8]. However, the SiMB method cannot be used to quantify silicate at low levels without the assistance of pre-concentration techniques. Ethyl acetate [9] and *n*-butanol [10] have been used to concentrate SiMY via liquid extraction prior to direct determination of SiMY in the organic phase or determination of SiMB after a reduction step. Sephadex gel [11] and a commercial solid phase extraction (SPE) cartridge [12] have been used for extraction of SiMB from ultra pure water samples. Silicate in seawater has been concentrated via the Magnesium Induced Co-precipitation (MAGIC) method, with a resulting ten-fold improvement in the limit of detection [1]. Most of these

* Corresponding author. Tel.: +1 727 553 1508; fax: +1 727 553 1189.
E-mail address: byrne@marine.usf.edu (R.H. Byrne).

0039-9140/$ – see front matter © 2011 Elsevier B.V. All rights reserved.
doi:10.1016/j.talanta.2011.11.019

pre-concentration technologies are laborious and time-consuming. Some are unsuitable for use in the field or are unsuitable for use with seawater. A recently reported electrochemical method based on detection of the silicomolybdic complex formed in acidic media has potential for long-term *in situ* deployments in seawater [13,14], but the 1 μM detection limit is high relative to needs of work in the oligotrophic ocean. Instrumentation such as Inductively Coupled Plasma–Atomic Emission Spectrometry (ICP–AES) [15], Ion Exclusion Chromatography–ICP–Mass Spectrometry (IEC–ICP–MS) [16] and IEC conductivity detection [17] have been used for sensitive determinations of silicate in seawater, but the analytical instrumentation is expensive and voluminous, and in many venues experienced operators may not be available.

Long pathlength absorbance spectrophotometry (LPAS) can reduce detection limits by increasing spectrophotometric pathlength. Through use of a flexible fluoropolymer material (AF-2400, Dupont) with a refractive index (1.29) smaller than that of water (1.33) [18], liquid core waveguides (LCW) are increasingly being used to enhance the sensitivity of spectrophotometric analyses [19–24]. Recently, Amornthammarong and Zhang [25] reported a liquid core waveguide spectrophotometric measurement of low-level silicate in natural waters. The analytical protocol produced SiMB, and poly-vinyl alcohol was added to prevent precipitation in the ammonium molybdate solution and improve the stability of the SiMB complex. The procedure of Amornthammarong and Zhang [25] is suitable for shipboard determination of silicate in surface seawater. However, the analysis time is comparatively lengthy (~15 min sample^{-1}) and, most importantly, the detection limit, (100 nM) is unexpectedly high for a 2 m LCW.

Flow injection analysis (FIA), which involves injection of a small volume of sample into a stream of reagent flowing through a detector, has the merits of simplicity, amenability to automation, high sample-throughput rate, and low risk of contamination [26]. FIA has been widely used for silicate measurement with short pathlength flow cells [27–31]. Korenaga and Sun [32] determined silicate with an FIA system composed of a laser diode and a thin flow-through cell constructed using a 10 cm polytetrafluoroethylene rod. However, it appears that FIA has never been used in combination with an LCW to achieve nanomolar detection limits for silicate.

Here we report a fast, sensitive, automated FIA method for the determination of low-level silicate concentrations, based on formation of SiMB. Optimization of analytical conditions for the FIA–LCW analysis involved investigation of reagent compositions and concentrations, injection loop volumes, mixing-coil lengths, and sample/reagent flow rates. The interference of phosphate (i.e., formation of a phosphomolybdate complex) was investigated and eliminated. The resulting method is well suited for shipboard/underway applications in marine science and in on-line industrial applications.

2. Experimental

2.1. Reagents

All chemicals used were reagent grade or better, purchased from Baker (www.mallbaker.com) or Sigma (www.sigmaaldrich.com) without further purification. Milli-Q water (www.Millipore.com), 18.2 MΩ cm, was used throughout. All solutions were prepared and stored in plastic containers to avoid potential contamination from glass vessels [33]. The stock silicate solution (1000 mg L^{-1}, Fisher), an atomic absorption reference standard solution, was stored in a plastic bottle. Molybdate solution (15 g L^{-1}, R1) was made by dissolving 3.75 g ammonium molybdate tetrahydrate in 250 mL of 100 mM diluted ULTREX II Ultrapure sulphuric acid. Oxalic acid solution (50 g L^{-1}, R2), prepared by dissolving 12.5 g of oxalic acid in 250 mL MQ water, was stored in an amber plastic bottle. Ascorbic acid solution (25 g L^{-1}, R3), prepared by dissolving 6.25 g of ascorbic acid in 250 mL MQ water, was stored in an amber plastic bottle at 4 °C. NaCl solution (0.7 M) was used as a matrix for salt-effect experiments.

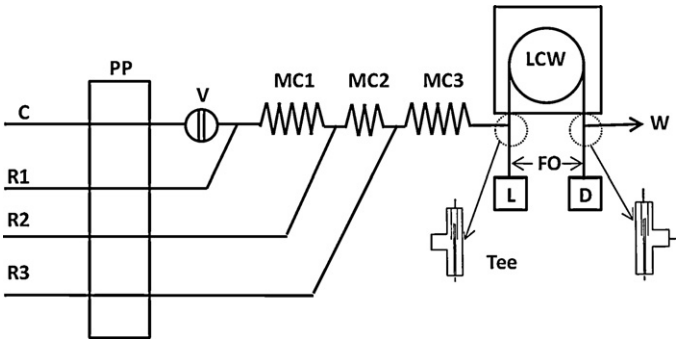

Fig. 1. Schematic diagram of the analytical system. C, carrier (MQ water or 0.7 M NaCl solution); R1, 0.012 M molybdate solution (15 g L^{-1} of $(NH_4)_6(Mo)_7O_2{\cdot}4H_2O$ in 100 mM H_2SO_4); R2, 0.56 M oxalic acid solution (50 g L^{-1} of $C_2H_2O_4$); R3, 0.14 M ascorbic acid solution (25 g L^{-1} $C_6H_8O_6$); PP, peristaltic pump; V, injection valve with 400 μL injection volume; MC 1, 2, 3: mixing coil 1 (80 cm), 2 (20 cm) and 3 (40 cm); LCW, liquid core waveguide (160 cm); FO, fiber optic; L, light source; D, detector; W, waste. The inset diagram shows details of the T connection.

2.2. Experimental arrangements

The experimental system (Fig. 1) utilized a four-channel peristaltic pump (www.ismatec.com) for delivery of sample and reagents. In order to simplify the system, all the channels were equipped with the same 1.02 mm inner diameter (i.d.) Tygon® tubing (www.coleparmer.com) and were operated at the same flow rate. Samples were injected through a six-port injection valve (www.vici.com) with a syringe or auto-sampler. Injected samples were mixed with reagents in three two-dimensionally serpentine *x*-plane-extended mixing coils (MC) [34], leading to the formation of SiMB, which was monitored in the LCW-based detector. The heart of the detector was a 160 cm length of Teflon AF-2400 LCW tubing (www.biogeneral.com) with an i.d. of 560 μm and an outer diameter (o.d.) of 800 μm. The LCW was coiled and placed in a black box to prevent introduction of ambient light into the LCW. A custom "T" connector allowed the coupling of 150 μm fiber optics (FO, www.polymicro.com) into the LCW and, via a ¼-28 thread connector (details shown in insert of Fig. 1), served as a portal for delivering liquid to the LCW via the Tygon® tubing described above. A detailed description of the system for coupling the tubing, LCW, and fiber optics can be found in the work of Yao and Byrne [35]. A tungsten lamp (www.avantes.com) driven at 5 V was used as the light source. A USB 4000 miniature fiber optic CCD spectrometer (www.oceanoptics.com) was used for absorbance measurements. Although SiMB has absorbance maxima at 660 and 810 nm, with the molar absorbance being much larger at 810 nm [8], in view of detector and lamp characteristics all absorbances were monitored at 660 nm. Detector output (intensity, *I*, of transmitted light) was acquired on a laptop PC. The detector count rate at 660 nm is converted to absorbance (*A*) via the following relationship, $A = \log (I_0 - I_{dark})/(I - I_{dark})$, where I_0 is the intensity (count rate) when the LCW is filled with the mixture of carrier and reagents, I_{dark} is the detector count rate when the lamp is turned off, and *I* is the intensity of light recorded while the sample is being monitored. A 10-point average (~0.4 s point^{-1}) was used to reduce signal noise from pump pulsation. Following the recommendation of Gimbert and Worsfold [23], the LCW was sequentially flushed with pure water, 1 M NaOH (10 mL), 1 M HCl (10 mL), and again with pure water (30 mL) prior to use and prior to storage.

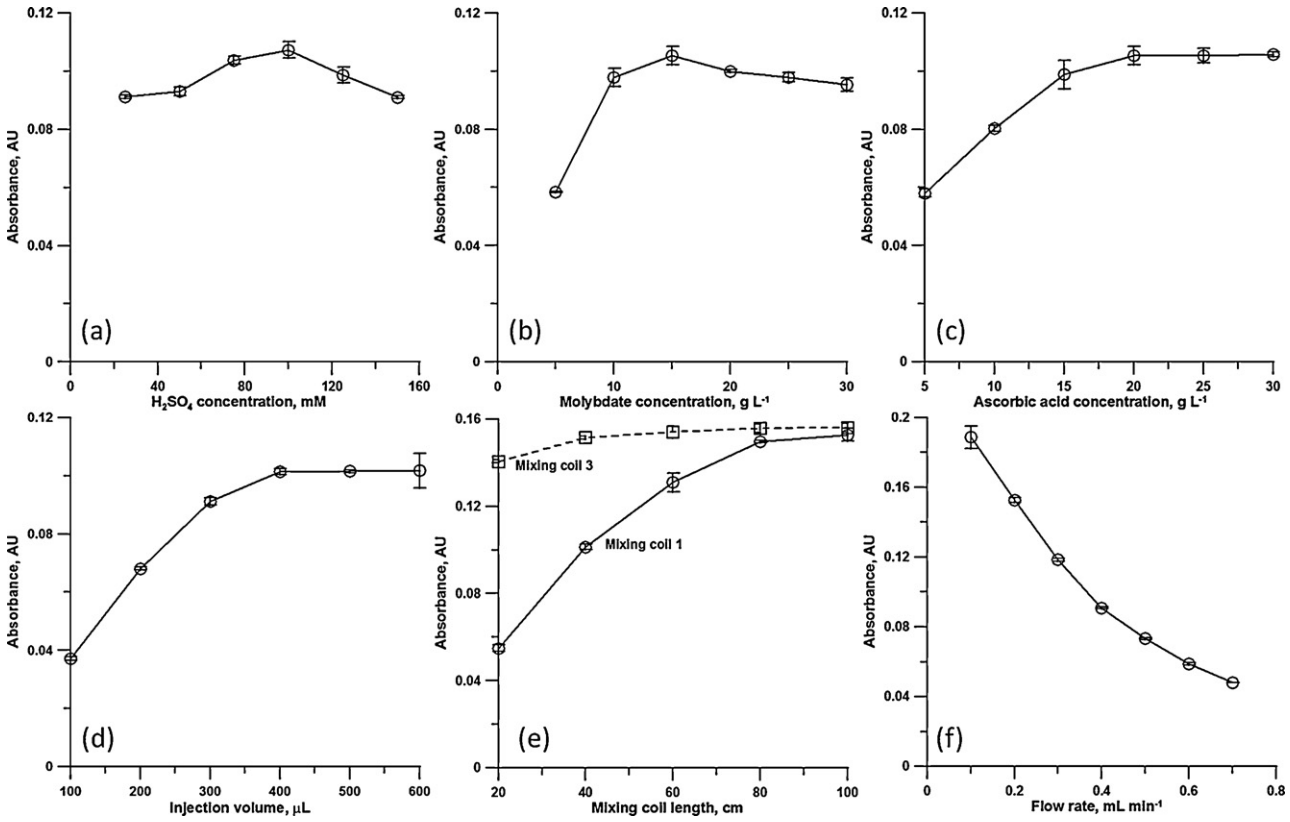

Fig. 2. Parameter optimization: Results are shown as an average ± the standard deviation (SD, $n = 3$). (a) Effect of H_2SO_4 concentration on absorbance. The H_2SO_4 concentration was varied between 25 and 150 mM, with molybdate concentration = 10 g L^{-1}, ascorbic acid concentration = 15 g L^{-1}, and oxalic acid concentration = 50 g L^{-1}. The injection volume was 400 μL, MC1 = 40 cm, MC2 = 20 cm, MC3 = 40 cm, and flow rate = 0.2 mL min^{-1}. (b) Effect of molybdate concentration on absorbance. The molybdate concentration was varied from 5 to 30 g L^{-1}, with H_2SO_4 concentration = 100 mM, ascorbic acid concentration = 15 g L^{-1}, and oxalic acid concentration = 50 g L^{-1}. The injection volume was 400 μL, MC1 = 40 cm, MC2 = 20 cm, MC3 = 40 cm, and the flow rate = 0.2 mL min^{-1}. (c) Effect of ascorbic acid concentration on absorbance. The ascorbic acid concentration was varied from 5 to 30 g L^{-1}, with H_2SO_4 concentration = 100 mM, molybdate concentration = 15 g L^{-1}, and oxalic acid concentration = 50 g L^{-1}. The injection volume was 400 μL, with MC1 = 40 cm, MC2 = 20 cm, MC3 = 40 cm, and flow rate = 0.2 mL min^{-1}. (d) Effect of injection volume on absorbance. Flow rate was varied from 100 to 600 μL, with H_2SO_4 concentration = 100 mM, molybdate concentration = 15 g L^{-1}, ascorbic acid concentration = 25 g L^{-1}, and oxalic acid concentration = 50 g L^{-1}. MC1 = 40 cm, MC2 = 20 cm, MC3 = 40 cm, and flow rate = 0.2 mL min^{-1}. (e) Effect of mixing-coil lengths on absorbance. MC1 and MC3 were varied from 20 to 100 cm, with H_2SO_4 concentration = 100 mM, molybdate concentration = 15 g L^{-1}, ascorbic acid concentration = 25 g L^{-1}, and oxalic acid concentration = 50 g L^{-1}. The injection volume was 400 μL, with flow rate = 0.2 mL min^{-1} and MC2 = 20 cm. For variations in MC1, the length of MC3 was 40 cm (solid line, circle symbols). For variations in MC3, the length of MC1 was 80 cm (dashed line, square symbols). (f) Effect of flow rate on absorbance. Flow rate was varied from 0.1 to 0.7 mL min^{-1}, with H_2SO_4 concentration = 100 mM, molybdate concentration = 15 g L^{-1}, ascorbic acid concentration = 25 g L^{-1}, and oxalic acid concentration = 50 g L^{-1}. The injection volume was 400 μL, with MC1 = 80 cm, MC2 = 20 cm, and MC3 = 40 cm.

3. Results and discussion

The influence of various parameters such as reagent composition, volume of the injection loop, lengths of the mixing coils, and rate of flow was investigated and optimized via univariate experimental design. A 0.89 μM silicate standard solution was used throughout the parameter-optimization procedures. Each sample was quantified three times, and the results were shown as an average ± the standard deviation (SD, $n = 3$). Although elevated temperature is beneficial for the SiMB reaction [27,29], all experiments were conducted at room temperature (~20 °C) to assess the performance of the analytical protocol for deployments in the field.

3.1. Influence of H_2SO_4 and molybdate concentration

Depending on pH, SiMY can exist in two isomeric forms: an α-isomer at pH 3.5–4.5 and a β-isomer at pH of 0.8–2.5 [8]. Therefore the effect of H_2SO_4 concentration (pH) on the colorimetric silicate measurement procedure needs to be optimized. As shown in Fig. 2(a), the highest SiMY signal was obtained with an H_2SO_4 concentration equal to 100 mM. This concentration was chosen for all further analyses. As the molar ratio of acid and molybdate is critical for both phosphate and silicate determinations [26], the influence of molybdate concentration on SiMB formation was also studied. For H_2SO_4 maintained at 100 mM, an optimal molybdate concentration, as shown in Fig. 2(b), is 15 g L^{-1} (~12 mM) and the [H]/[Mo] ratio is ~16.7.

3.2. Influence of ascorbic acid concentration

Both stannous chloride and ascorbic acid have been widely used as reductants for the SiMB reaction. Although the reaction with stannous chloride is a faster reaction and has a smaller temperature effect, ascorbic acid was chosen because of easier reagent preparation, improved linearity, and lower blank values [27]. The influence of ascorbic acid concentration on the SiMB reaction was studied within the range of 5–30 g L^{-1}. As shown in Fig. 2(c), SiMB absorbance increased with ascorbic acid concentration up to 20 g L^{-1}. Beyond this concentration there was no significant variation in observed signals. A 25 g L^{-1} ascorbic acid concentration was used in all subsequent work.

3.3. Influence of injection volume

The sample injection volume controls the silicate concentration in the reagent–sample mixture and therefore the final absorbance

signal. Injection volumes between 100 and 600 μL were evaluated in the optimization process. Signal increases were observed for injection volumes up to 400 μL (Fig. 2(d)). Peak broadening and reduced reproducibility was observed for injection volumes larger than 500 μL. The existence of peak broadening suggests that silicate was excessive in the mid-portion of the sample zone, with complete reaction being assured only at the leading and trailing edges of the sample zone. As such, 400 μL was chosen as the injection volume for all subsequent measurements.

3.4. Effect of mixing coil (MC) length

Since the invention of FIA, a range of reactor geometries has been investigated [29]. The two-dimensionally serpentine *x*-plane-extended MC chosen in this study has low dispersion and good reproducibility and is simple to fabricate. A detailed comparison of this and other reactor geometries is found in the work of Waiz at al. [34]. The influence of mixing coil lengths for coils MC1 and MC3 is shown in Fig. 2(e). The MC2 length (20 cm) was not varied. This choice, in conjunction with a sample flow rate of 0.2 mL min^{-1}, resulted in an elapsed time of 30 s between addition of oxalic acid in R2 and addition of ascorbic acid in R3. Fig. 2(e) shows that lengthening MC1 beyond 80 cm resulted in only a modest enhancement of SiMY absorbance. Therefore, a length of 80 cm was chosen to achieve a balance between improved detection sensitivity and improved sample throughput. Signal enhancement for MC3 length greater than 40 cm was small. Accordingly, the chosen length of MC3 was 40 cm.

3.5. Influence of flow rate

High flow rates can reduce the reaction extent for a target analyte, while insufficient flow rates can result in higher dispersion and peak broadening. As illustrated in Fig. 2(f), absorbances uniformly decreased as flow rate was increased beyond 0.1 mL min^{-1}. However, measurements at 0.1 mL min^{-1} resulted in some peak broadening and, importantly, a somewhat degraded rate of sample analysis. A flow rate of 0.2 mL min^{-1} was therefore chosen, considering both sensitivity and sample throughput.

3.6. Phosphate interference study

Phosphate and silicate have similar reaction chemistries with molybdate in acidic solutions. As such, the interferences of each on the other have been investigated in previous works [25–27,36]. For silicate determinations, the presence of oxalic acid is used to avoid reduction of excess molybdate and to suppress the development of absorbing phosphomolybdate complexes in solution [25]. The latter process can be quite important for analysis of seawater. Samples containing 0.89 μM silicate and 0.89 μM silicate + 8 μM phosphate were analyzed at a flow rate of 0.2 mL min^{-1}. The added phosphate was far larger than normal phosphate concentrations in seawater (i.e., seawater phosphate concentrations are ≤3.6 μM). Fig. 3 shows that 50 g L^{-1} oxalic acid solution is more than sufficient for eliminating phosphate interference in low-level silicate determinations. Samples of natural seawater (salinity 35.5) without and with 8 μM added phosphate were analyzed, producing absorbances equal to 0.1781 ± 0.0034 and 0.1805 ± 0.0067, respectively. As the difference between these absorbances is not statistically significant based on the one tail *t*-test at the 95% confidence level (*t*-calculated is 0.41, lower than *t*-critical 2.92), the interference from 8 μM phosphate for our reaction conditions is negligible. This result is in accordance with standard methods and reported protocols for seawater analysis [6,8,25].

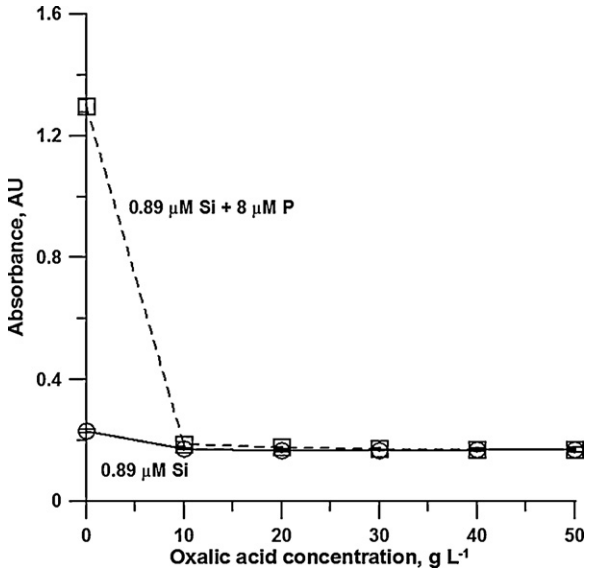

Fig. 3. Elimination of phosphate interference using oxalic acid. The oxalic acid concentration was varied from 0 to 50 g L^{-1} at H_2SO_4 concentration = 100 mM, molybdate concentration = 15 g L^{-1}, and ascorbic acid concentration = 25 g L^{-1}. The injection volume was 400 μL, with MC1 = 80 cm, MC2 = 20 cm, MC3 = 40 cm, and flow rate = 0.2 mL min^{-1}.

3.7. Influence of salinity

The experiments described above were conducted using MQ water as the carrier, and all the samples were prepared in pure water. However, salinity can exert important effects on the analytical protocol for determination of dissolved silica. Schlieren effects can result from the refractive index difference between the carrier (e.g., MQ water) and sample (e.g., seawater) [37]. The Schlieren effect can be overcome by matching the salinity of carrier and sample [26]. Therefore, to compensate for reflective index differences, a 0.7 M NaCl solution was used as the carrier for seawater analyses. This was done in view of the fact that calibration curves obtained in MQ water and 0.7 M NaCl solution were identical (Fig. 4), indicating that there are no significant medium concentration effects between MQ water and 0.7 M NaCl. The difference

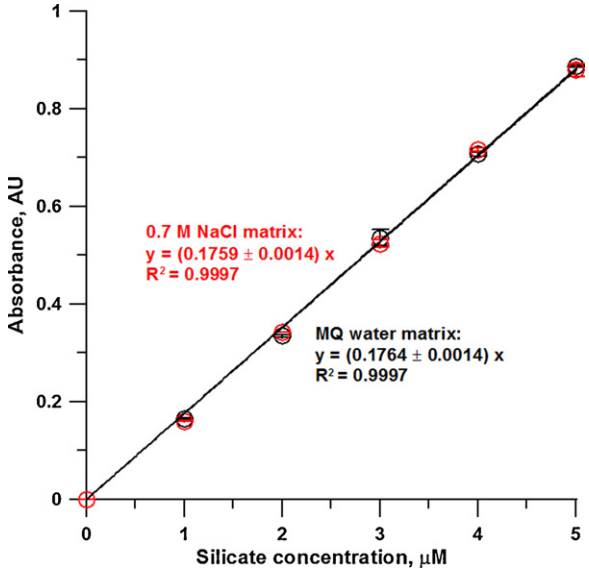

Fig. 4. Calibration curves in MQ water and 0.7 M NaCl using the optimized parameters.

Table 1
Recommended analytical parameters.

Parameter	Range of tested values	Selected value
H_2SO_4 concentration, mM	25–150	100
Molybdate concentration, g L^{-1}	5–30	15
Ascorbic acid, g L^{-1}	5–30	25
Oxalic acid, g L^{-1}	0–50	50
Injection volume, μL	100–600	400
Length of mixing coil 1, cm	20–100	80
Length of mixing coil 2, cm	–	20
Length of mixing coil 3, cm	20–100	40
Flow rate, mL min^{-1}	0.1–0.7	0.2

between the Grasshoff et al. [8] observation of a substantial salinity effect (the molar absorptivity at 810 nm of the SiMB in pure water, 22,000 M^{-1} cm^{-1}, was reported to be higher than the molar absorptivity of SiMB in ocean water, 19,000 M^{-1} cm^{-1}) and the absence of such an effect in the present work is likely attributable to dilution of the sample and carrier. In the current work, the carrier is diluted by three reagents and the reaction occurs in a matrix with only one-fourth its original salinity. At such low salinities/concentrations, medium effects and refractive index affects appear to be negligible. This interpretation was further substantiated by observation of calibration curves for three seawater samples collected from the Gulf of Mexico (salinity 35–36). The average slope obtained for these samples was 0.1741 ± 0.0015 Abs μM^{-1}, in good agreement with the slopes of calibration curves obtained in MQ water (0.1764 ± 0.0014 Abs μM^{-1}) and in the 0.7 M NaCl matrix (0.1759 ± 0.0014 Abs μM^{-1}). Amornthammarong and Zhang [25] reported similar calibration slope results with minor salinity changes (i.e., the slope was 0.1054 Abs μM^{-1} at salinity 0 and 0.1046 Abs μM^{-1} at salinity 9).

3.8. Analytical figures of merit

Under the optimized conditions (Table 1), calibration curves for two distinct matrices obtained over a 0–5 μM concentration range (Fig. 4) show insignificant concentration effects. Fig. 4 calibration line for silicate in MQ water (with MQ water as the carrier) is collinear with the calibration line for silicate in 0.7 M NaCl (where 0.7 M NaCl is the carrier). The range of silicate concentrations for Fig. 4 calibration curve is appropriate for surface seawater in oligotrophic regions. Sample throughput for the optimized conditions is 12 h^{-1} at a flow rate of 0.2 mL min^{-1}.

The detection limit (DL) was calculated as 3 times the SD for measurement of low-concentration samples (250 nM, $n = 9$) divided by the calibration curve slopes in pure water and 0.7 M NaCl (0.1764 ± 0.0014 and 0.1759 ± 0.0014 Abs μM^{-1}). DLs were 7.2 and 9.0 nM for pure water and NaCl at the ionic strength of seawater (equivalent to absorbances of 0.0013 and 0.0016), respectively. Standard deviations of blanks were not used because carrier absorbances and blank absorbances were identical; the blank value was essentially zero with a very low standard deviation. The relative standard deviations (RSDs) for repetitive determinations of 250 nM silicate in MQ water and seawater were 1.50% ($n = 7$) and 1.51% ($n = 7$). The limits of detection and relative standard deviations demonstrated in this work show that the FIA–LCW protocols are appropriate for determination of silicate in both industrial and marine applications.

3.9. Application

The protocol developed in this study was used for determination of silicate in seawater samples collected in the Gulf of Mexico, July 19–20, 2011. After collection via an underway sampling system, seawater samples were kept in a refrigerator (4 °C) in the dark and then analyzed in the laboratory within 2 days. Measured silicate concentrations in the surface water ranged from 0.5 to 8 μM, with near shore coastal waters having higher concentrations than waters from the offshore region. These seawater samples were also analyzed with the standard silicate protocol [8] using a 10 cm cell. A comparison of the two methods exhibited excellent agreement. Silicate measured with the FIA–LCW method = $(0.9908 \pm 0.0071) \times$ silicate measured with the classic silicate measurement method ($R^2 = 0.9991$, $n = 19$). As such, it is seen that FIA–LCW measurements are appropriate over the range of silicate concentrations that can be observed with standard silicate protocols, and FIA–LCW procedures extend silicate measurement capabilities to concentrations that are too low to be accessible with standard protocols.

4. Conclusion

The combination of a long pathlength LCW and a compact fiber optic-based CCD spectrometer provide a very sensitive, simple, and robust approach for flow injection analysis of silicate at nanomolar levels. FIA–LCW procedures exhibit good reproducibility (RSD ~ 1.5%), and relative to the pioneering LCW-based silicate analysis protocol of Amornthammarong and Zhang [25], the protocol developed in this study has a much-improved sensitivity (DL = 10 nM vs. 100 nM), and sample throughput (5 min $sample^{-1}$ vs. 15 min $sample^{-1}$). The method exhibits no significant salinity effects. The experimental setup can be easily modified for on-line measurement of trace silicate in ultra pure water (industrial applications) and shipboard/underway measurements in seawater (marine science applications).

Acknowledgements

This work was supported by the Office of Naval Research: Grants N00014-03-1-0612 and N00014-10-1-0787. Dr. R.T. Masserini Jr. and W. Abbott are thanked for collection of seawater samples.

References

[1] P. Rimmelin-Maury, T. Moutin, B. Queguiner, Anal. Chim. Acta 587 (2007) 281–286.
[2] M.A. Brzezinski, D.M. Nelson, Deep-Sea Res. I 42 (1995) 1215–1237.
[3] J.-C. Marty, J. Chiaverini, M.-D. Pizay, B. Avril, Deep-Sea Res. II 49 (2002) 1965–1985.
[4] K. Leblanc, C.E. Hare, P.W. Boyd, K.W. Bruland, B. Sohst, S. Pickmere, M.C. Lohan, K. Buck, M. Ellwood, D.A. Hutchins, Deep-Sea Res. I 52 (2005) 1842–1864.
[5] A. Sabarudin, M. Oshima, N. Ishii, S. Motomizu, Talanta 60 (2003) 1277–1285.
[6] US Environmental Protection Agency, Method 366.0, 1997.
[7] APHA, AWWA, WEF, Standard Methods for the Examination of Water and Wastewater, 4500-Si, 1995.
[8] H.P. Hansen, F. Koroleff, in: K. Grasshoff, M. Kremling, Ehrhardt (Eds.), Methods of Seawater Analysis, 3rd ed., Wiley-VCH, 1999, pp. 193–199.
[9] D.R. Schink, Anal. Chem. 37 (1965) 764–765.
[10] M. Brzezinski, D.M. Nelson, Mar. Chem. 19 (1986) 139–151.
[11] K. Yoshimura, M. Motomura, T. Tarutani, T. Shimono, Anal. Chem. 56 (1984) 2342–2345.
[12] Y. Peng, M. Zhang, J. Ma, D. Yuan, Fenxi Huaxue 37 (2009) 1258–1262.
[13] M. Lacombe, V. Garcon, M. Comtat, L. Oriol, J. Sudre, D. Thouron, N.L. Bris, C. Provost, Mar. Chem. 106 (2007) 489–497.
[14] M. Lacombe, V. Garcon, D. Thouron, N.L. Bris, M. Comtat, Talanta 77 (2008) 744–750.
[15] K. Abe, Y. Watanabe, J. Ocean 48 (1992) 283–292.
[16] A. Hioki, J.W.H. Lam, J.W. McLaren, Anal. Chem. 69 (1997) 21–24.
[17] H. Li, F. Chen, J. Chromatogr. A 874 (2000) 143–147.
[18] R.H. Byrne, W. Yao, E. Kaltenbacher, R.D. Waterbury, Talanta 50 (2000) 1307–1312.
[19] R.D. Waterbury, W. Yao, R.H. Byrne, Anal. Chim. Acta 357 (1997) 99–102.
[20] W. Yao, R.H. Byrne, R.D. Waterbury, Environ. Sci. Technol. 32 (1998) 2646–2649.
[21] M.R. Callahan, J.B. Rose, R.H. Byrne, Talanta (2002) 891–898.
[22] T. Dallas, P.K. Dasgupta, Trends Anal. Chem. 23 (2004) 385–392.
[23] L. Gimbert, P.J. Worsfold, Trends Anal. Chem. 26 (2007) 914–930.
[24] L.R. Adornato, E.A. Kaltenbacher, D.R. Greenhow, R.H. Byrne, Environ. Sci. Technol. 41 (2007) 4045–4052.
[25] N. Amornthammarong, J.-Z. Zhang, Talanta 79 (2009) 621–626.

[26] J. Ma, D. Yuan, M. Zhang, Y. Liang, Talanta 78 (2009) 315–320.
[27] J. Thomsen, K.S. Johnson, R.L. Petty, Anal. Chem. 55 (1983) 2378–2382.
[28] J. Saurina, S. Hernández-Cassou, Analyst 120 (1995) 2601–2604.
[29] J. Floch, S. Blain, D. Birot, P. Treguer, Anal. Chim. Acta 377 (1998) 157–166.
[30] M. Yaqoob, A. Nabi, P.J. Worsfold, Anal. Chim. Acta 519 (2004) 137–142.
[31] B. Hales, A.V. Geen, T. Takahashi, Limnol. Oceanogr. Methods 2 (2004) 91–101.
[32] T. Korenaga, F. Sun, Anal. Chim. Acta 318 (1996) 195–202.
[33] J.-Z. Zhang, C.J. Fischer, P.B. Ortner, Water Res. 33 (1999) 2879–2882.
[34] S. Waiz, B.M. Cedillo, S. Jambunathan, S.G. Hohnholt, P.K. Dasgupta, D.K. Wolcott, Anal. Chim. Acta 428 (2001) 163–171.
[35] W. Yao, R.H. Byrne, Talanta 48 (1999) 277–282.
[36] J. Ma, D. Yuan, Y. Liang, Mar. Chem. 111 (2008) 151–159.
[37] I.D. McKelvie, D.M.W. Peat, G.P. Matthews, P.J. Worsfold, Anal. Chim. Acta 351 (1997) 265–271.